# Impact of B4C co-sputtering on structure and optical performance of Cr/Sc multilayer X-ray mirrors

Naureen Ghafoor, Fredrik Eriksson, Aquila Andrew, Gullikson Eric, Schäfers Franz, Grzegorz Greczynski and Jens Birch


Ghafoor, N., Eriksson, F., Andrew, A., Eric, G., Franz, S., Greczynski, G., Birch, J., (2017), Impact of B4C co-sputtering on structure and optical performance of Cr/Sc multilayer X-ray mirrors, *Optics Express*, 25(15). https://doi.org/10.1364/oe.25.018274

Original publication available at:
https://doi.org/10.1364/oe.25.018274

# Impact of $B_4C$ co-sputtering on structure and optical performance of Cr/Sc multilayer X-ray mirrors

**NAUREEN GHAFOOR,[1,*] FREDRIK ERIKSSON,[1] ANDREW AQUILA,[2] ERIC GULLIKSON,[3] FRANZ SCHÄFERS,[4] GREZGORZ GRECZYNSKI,[1] AND JENS BIRCH[1]**

[1] *Department of Physics, Chemistry, and Biology, IFM, Linköping University, Sweden*
[2]*SLAC National Accelerator Laboratory, 2575 Sand Hill Road, Menlo Park, California 94025, USA*
[3] *Center for X-Ray Optics, Lawrence Berkeley National Lab, Berkeley, CA 94720, USA*
[4]*Institute for Nanometre Optics and Technology Helmholtz Zentrum Berlin für Materialien und Energie, Albert-Einstein-Str. 15, 12489 Berlin, Germany*
[*]*naureen.ghafoor@liu.se*

**Abstract:** The influence of $B_4C$ incorporation during magnetron sputter deposition of Cr/Sc multilayers intended for soft X-ray reflective optics is investigated. Chemical analysis suggests formation of metal: boride and carbide bonds which stabilize an amorphous layer structure, resulting in smoother interfaces and an increased reflectivity. A near-normal incidence reflectivity of 11.7 %, corresponding to a 67% increase, is achieved at $\lambda$=3.11 nm upon adding 23 at.% (B+C). The advantage is significant for the multilayer periods larger than 1.8 nm, where amorphization results in smaller interface widths, for example, giving 36% reflectance and 99.89% degree of polarization near Brewster angle for a multilayer polarizer. The modulated ion-energy-assistance during the growth is considered vital to avoid intermixing during the interface formation even when B+C are added.



**OCIS codes:** (340.7480) X-rays, soft X-rays, extreme ultraviolet (EUV); (310.6860) Thin films, optical properties; (310.4165) Multilayer design; (340.7470) X-ray mirrors; (240.1485) Buried interfaces.

## References and links

1. J. T. W. Barbee, "Multilayers for X-ray optics," Opt. Eng. **25**, 893 (1986).
2. E. Spiller, A. Segmüller, J. Rife, and R. P. Haelbich, "Controlled fabrication of multilayer soft-x-ray mirrors," Applied Physics Letters **37**, 1048 (1980).
3. E. Louis, A. E. Yakshin, T. Tsarfati, and F. Bijkerk, "Nanometer interface and materials control for multilayer EUV-optical applications," Progress in Surface Science **86**, 255 (2011).
4. M. Bertilson, O. v. Hofsten, U. Vogt, A. Holmberg, and H. M. Hertz, "High-resolution computed tomography with a compact soft x-ray microscope," Opt. Express **17**, 11057 (2009).
5. M. S. Bibishkin, N. I. Chkhalo, A. A. Fraerman, A. E. Pestov, K. A. Prokhorov, N. N. Salashchenko, and Y. A. Vainer, "Ultra-short period X-ray mirrors: Production and investigation," Nucl Instrum Meth A **543**, 333 (2005).
6. S. Yulin, *"Multilayer Coatings for EUV/Soft X-ray Mirrors,"* in *Optical Interference Coatings*, N. Kaiser, and H. K. Pulker, eds. pp. 281-307 (Springer Berlin Heidelberg, 2003).
7. F. Schäfers, H.-C. Mertins, F. Schmolla, I. Packe, N. N. Salashchenko, and E. A. Shamov, "Cr/Sc multilayers for the soft-x-ray range," Appl. Opt. **37**, 719 (1998).
8. A. F. G. Leontowich, A. Aquila, F. Stellato, R. Bean, H. Fleckenstein, M. Prasciolu, M. Liang, D. P. DePonte, A. Barty, F. Wang, J. Andreasson, J. Hajdu, H. N. Chapman, and S. Bajt, "Characterizing the focus of a multilayer coated off-axis parabola for FLASH beam at $\lambda$ = 4.3 nm," *Proc. SPIE 8777, Damage to VUV, EUV, and X-ray Optics IV; and EUV and X-ray Optics:* Synergy between Laboratory and Space III, 87770T (May 3, 2013).

9. F. Eriksson, G. A. Johansson, H. M. Hertz, E. M. Gullikson, U. Kreissig, and J. Birch, "14.5% near-normal incidence reflectance of Cr Sc x-ray multilayer mirrors for the water window," Opt. Lett. **28**, 2494 (2003).
10. T. Kuhlmann, S. Yulin, T. Feigl, N. Kaiser, T. Gorelik, U. Kaiser, and W. Richter, "Chromium–scandium multilayer mirrors for the nitrogen K α line in the water window region," Applied Optics **41**, 2048 (2002).
11. K. A. Gschneidner Jr, "CHAPTER 9 - Alloys and Intermetallic Compounds," in *Scandium: Its Occurrence, Chemistry Physics, Metallurgy, Biology and Technology*(Academic Press, 1975), pp. 252-322.
12. N. Ghafoor, F. Eriksson, A. S. Mikhaylushkin, I. A. Abrikosov, E. M. Gullikson, U. Kressig, M. Beckers, L. Hultman, and J. Birch, "Effects of O and N impurities on the nanostructural evolution during growth of Cr/Sc multilayers," Journal of Materials Research **24**, 79 (2009).
13. N. Ghafoor, F. Eriksson, P. O. Å. Persson, L. Hultman, and J. Birch, "Effects of ion-assisted growth on the layer definition in Cr/Sc multilayers," Thin Solid Films **516**, 982 (2008).
14. E. Meltchakov, V. Vidal, H. Faik, M. J. Casanove, and B. Vidal, "Performance of multilayer coatings in relationship to microstructure of metal layers. Characterization and optical properties of Mo/Si multilayers in extreme ultra-violet and x-ray ranges," Journal of Physics: Condensed Matter **18**, 3355 (2006).
15. J. Peng, W. Li, Q. Huang, and Z. Wang, "Microstructure evolution with varied layer thickness in magnetron-sputtered Ni/C multilayer films," Scientific Reports **6**, 31522 (2016).
16. A. Haase, S. Bajt, P. Hönicke, V. Soltwisch, and F. Scholze, "Multiparameter characterization of subnanometre Cr/Sc multilayers based on complementary measurements," Journal of Applied Crystallography **49**, 2161 (2016).
17. A. Guggenmos, M. Jobst, M. Ossiander, S. Radünz, J. Riemensberger, M. Schäffer, A. Akil, C. Jakubeit, P. Böhm, S. Noever, B. Nickel, R. Kienberger, and U. Kleineberg, "Chromium/scandium multilayer mirrors for isolated attosecond pulses at 145 eV," Opt. Lett. **40**, 2846 (2015).
18. A. Guggenmos, R. Rauhut, M. Hofstetter, S. Hertrich, B. Nickel, J. Schmidt, E. M. Gullikson, M. Seibald, W. Schnick, and U. Kleineberg, "Aperiodic CrSc multilayer mirrors for attosecond water window pulses," Opt. Express **21**, 21728 (2013).
19. A. Guggenmos, S. Radünz, R. Rauhut, M. Hofstetter, S. Venkatesan, A. Wochnik, E. M. Gullikson, S. Fischer, B. Nickel, C. Scheu, and U. Kleineberg, "Ion polished Cr/Sc attosecond multilayer mirrors for high water window reflectivity," Opt. Express **22**, 26526 (2014).
20. S. a. Bajt, J. B. Alameda, J. T. W. Barbee, W. M. Clift, J. A. Folta, B. Kaufmann, and E. A. Spiller, "Improved reflectance and stability of Mo-Si multilayers," OPTICE **41**, 1797 (2002).
21. C. Burcklen, S. de Rossi, E. Meltchakov, D. Dennetière, B. Capitanio, F. Polack, and F. Delmotte, "High-reflectance magnetron-sputtered scandium-based x-ray multilayer mirrors for the water window," Opt. Lett. **42**, 1927 (2017).
22. E. M. Gullikson, F. Salmassi, A. L. Aquila, and F. Dollar, "Progress in short period multilayer coatings for water window applications," in *8th International Conference on the Physics of X-Ray Multilayer Structures (PXRMS), oral presentation*, (Sapporo, Japan, 2006).
23. M. Prasciolu, A. F. G. Leontowich, K. R. Beyerlein, and S. Bajt, "Thermal stability studies of short period Sc/Cr and Sc/B4C/Cr multilayers," Applied Optics **53**, 2126 (2014).
24. E. M. G. B.L. Henke, and J.C. Davis, "X-ray interactions: photoabsorption, scattering, transmission, and reflection at E=50-30000 eV, Z=1-92,"Atomic Data and Nuclear Data Tables Vol. 54 (no.2), ed. ((July 1993)).
25. Q. Huang, J. Fei, Y. Liu, P. Li, M. Wen, C. Xie, P. Jonnard, A. Giglia, Z. Zhang, K. Wang, and Z. Wang, "High reflectance Cr/V multilayer with B4C barrier layer for water window wavelength region," Opt. Lett. **41**, 701 (2016).
26. Y. Tu, "Multilayer monochromators for EUV and X-ray optics and the interface characterization," PhD Thesis Chemical Physics [physics.chem-ph]. Universit de Pierre et Marie Curie - Paris VI, 66-68 (2015).
27. A. Patelli, J. Ravagnan, V. Rigato, G. Salmaso, D. Silvestrini, E. Bontempi, and L. E. Depero, "Structure and interface properties of Mo/B4C/Si multilayers deposited by rf-magnetron sputtering," Applied Surface Science **238**, 262 (2004).
28. H. J. Whitlow, C. S. Petersson, K. J. Reeson, and P. L. F. Hemment, "Mass-dispersive recoil spectrometry studies of oxygen and nitrogen redistribution in ion-beam-synthesized buried oxynitride layers in silicon," Applied Physics Letters **52**, 1871 (1988).
29. M. S. Jansson, "CONTES, Conversion of Time-Energy Spectra - a Program for ERDA Data Analysis, Uppsala University, (2004).
30. G. Greczynski, and L. Hultman, "C 1s Peak of Adventitious Carbon Aligns to the Vacuum Level: Dire Consequences for Material's Bonding Assignment by Photoelectron Spectroscopy," ChemPhysChem, **18**, 12 (2017).
31. N. Fairly, "XPS lineshapes and Curve Fitting " in *Surface Analysis by Auger and X-ray Photoelectron Spectroscopy*, D. B. J. Grant, ed. ( IM Publications, Chichester UK,, 2003), pp. 397- 398.
32. D. L. Windt, "IMD;software for modeling the optical properties of multilayer films," Comput. Phys. **12**, 360 (1998).
33. F. Schäfers, H.-C. Mertins, A. Gaupp, W. Gudat, M. Mertin, I. Packe, F. Schmolla, S. Di Fonzo, G. Soullié, W. Jark, R. Walker, X. Le Cann, R. Nyholm, and M. Eriksson, "Soft-x-ray polarimeter with multilayer optics: complete analysis of the polarization state of light," Applied Optics **38**, 4074 (1999).
34. T. Kenmotsu, T. Kawamura, T. Ono, and Y. Yamamura, "Dynamical simulation for sputtering of B4C," Journal of Nuclear Materials **258–263, Part 1**, 729 (1998).
35. T. Ono, T. Kawamura, K. Ishii, and Y. Yamamura, "Sputtering yield formula for B4C irradiated with monoenergetic ions at normal incidence," Journal of Nuclear Materials **232**, 52 (1996).

36. F. Eriksson, N. Ghafoor, S. Franz, E. M. Gullikson, S. Aouadi, S. Rohde, L. Hultman, and J. Birch, "Atomic scale interface engineering by modulated ion-assisted deposition applied to soft x-ray multilayer optics," Applied Optics **47**, 4196 (2008).
37. V. N. I. o. S. a. T. NIST X-ray Photoelectron Spectroscopy Database, Gaithersburg, 2012); http://srdata.nist.gov/xps/. Accessed: 2017-05-07]. .
38. K. E. Lee, J. Y. Lee, M. J. Park, J. H. Kim, C. B. Lee, and C. O. Kim, "Preparation of boron carbide thin films for HDD protecting layer," Journal of Magnetism and Magnetic Materials **272–276, Part 3**, 2197 (2004).

## 1. Introduction

A vital component in advancing the instrumentation in EUV and soft X-ray based lithographic tools, microscopes, solar telescopes, and time-resolved attosecond spectroscopy is normal-incidence multilayer X-ray optics. Multilayer mirrors with compositional modulation, providing high optical contrast for the desired reflected wavelength, have proven to serve as bright, highly dispersive, and efficient reflective optics [1-4]. The bottleneck in obtaining higher reflectivities, closer to the theoretically predicted values, in almost all chosen materials systems, is the fabrication of hundreds of nm to sub-nm thin layers with atomically flat and abrupt interfaces [5, 6].

Cr/Sc multilayers are often the most suitable structures to use as soft X-ray mirrors in water-window applications in-between C and Sc absorption edges [6-10]. Two facts related to Cr/Sc multilayers are that Cr and Sc do not form any intermetallic phase [11] at the interfaces, and that both Cr and Sc layers attain an amorphous structure below ~ 1.8 nm period [10, 12, 13]. The latter is a consequence of total energy minimization by eliminating high energy crystalline interfaces in favour of disordered ones, at the expense of forming an amorphous structure also in the interior of the layers [12]. When grown with multilayer periodicities larger than $\Lambda > 1.8$ nm, both Cr and Sc spontaneously transforms into nanocrystalline layers. In general, crystallization is a serious issue since crystallites increase high spatial frequency interfacial roughness resulting in a poor reflectivity performance [14, 15]. The impact is severe on optics requiring larger periodicities such as polarizers and broadband mirrors, essential to polarimetry and to shape attosecond pulses [16-18].

Successful experiments have been made to grow smooth interfaces in Cr/Sc multilayers with periods > 1.8 nm using ion beam deposition techniques as well as by the use of so called “diffusion barrier layers”. For example, Guggenmos et al. demonstrated that ion beam sputtering using 400 eV Kr ions (yielding sputtered Sc and Cr atoms with kinetic energies of about 10 eV) was the best trade-off for an optimized layer growth of defect free, dense, and smooth layers with abrupt interfaces [19]. Additionally, after every $10^{th}$ period, ion polishing was applied using 50 eV Kr ions (for 60 s at 31° normal incidence angle) to minimize roughness accumulation and ensure smoother interfaces. While providing a high degree of process control, optimization of ion energies and the ion-polishing steps makes the ion beam sputtering technique rather elaborate with relatively low overall low deposition rates (~0.05 nm/s). However, due to its better process control the technique was preferred over “diffusion barrier layers” [17, 19].

The concept of diffusion barrier layers is mainly to introduce a third component layer, often $B_4C$, in-between the main constituent layers to avoid intermixing at the interfaces which would reduce the optical contrast in the multilayers. The concept was first introduce for Mo/Si multilayers where the presence of sub-nm thin $B_4C$ layers, preferably on Mo-on-Si interfaces, was found to effectively hinder molybdenum silicide formation and provide higher optical contrast for EUV reflection [20]. In the soft X-ray regime, particularly for near-normal incidence soft X-ray mirrors where individual layers are sub-nm thin and consequently has even more stringent demands on absolute thickness accuracy, reproducibility, and interface perfection, the introduction of barrier layers is not straight forward. Nevertheless, ultrathin interleaved $B_4C$ layers have shown significantly improved interface definition in magnetron sputtered Cr/Sc multilayers [21-23]. Gullikson et al [22, 24] reported 32.1% near-normal-

incidence reflectivity at 3.11 nm wavelength for Cr/$B_4C$/Sc multilayers. Here, ~0.2 nm thin $B_4C$ layers were sequentially deposited only on the top of Cr layers.

Owing to the fact that thin interleaved $B_4C$ layers unambiguously have turned to be beneficial in obtaining highly reflective multilayers for a wide range of materials systems and wavelengths, fundamental understanding of the decisive role of $B_4C$ in restructuring interfaces and/or optical contrast in multilayer structures is needed [22, 25, 26]. How interleaved $B_4C$ layers affect the interfaces is not trivial to determine in nearly amorphous sub-nm thin layers with the existing experimental techniques. In short period Cr/Sc multilayers ($\Lambda < 1.8$ nm), they are assumed to act as barriers against displacements of atoms across the interfaces, i.e., to prevent intermixing, and thus yielding chemically abrupt interfaces. On the other hand, $B_4C$ layers are known to reduce the adatom surface mobility in e.g., Mo/$B_4C$/Si/$B_4C$ multilayers, increasing the interface roughness replication effect [27]. Since, interface flatness is equally desired as interface abruptness for high reflectance of the multilayer mirrors, essential measures must be taken, such as e.g. bombardment of the growing film by energetic particles (ions or atoms) to reduce such interface morphology replication.

In this paper, the investigations are focused on magnetron sputtered Cr/Sc multilayers deposited using *continuous* incorporation of $B_4C$ into both Cr and Sc layers. Different high flux, low energy ion assistance schemes have been implemented to elucidate the impact of $B_4C$ on the multilayer reflectivity performance. The effect of co-sputtering of $B_4C$ is demonstrated for a wide range of multilayer periodicities ($0.9 \leq \Lambda \leq 4.5$ nm) including the amorphous-crystalline transition at a period of 1.8 nm. The role of $B_4C$ in defining the multilayer structures i.e., if the effect is merely a smoothening of interfaces through stimulated amorphization or a reduced interlayer mobility of metal atoms, providing more abrupt interfaces, is investigated. Multiple characterization techniques are used to correlate the growth parameters, particularly the usage of a high flux low energy ion bombardment and the distribution of $B_4C$, with structural morphology and optical performance of the multilayers.

## 2. Growth and characterization details

### *2.1 Modulated ion-assisted growth during co-sputtering of $B_4C$*

The multilayers were deposited using an unbalanced dc-magnetron sputter deposition system with 75mm diameter Cr and Sc targets. The major upgrade of the system, since it was last described [13], is an addition of a 50 mm diameter sputtering source to enable $B_4C$ co-sputtering during multilayer deposition. All three targets face the substrate at an angle of 25° from the substrate normal. Fast acting computer controlled shutters in front of the Cr and Sc targets are used to sequentially deposit Cr and Sc whereas a manual shutter is used to control the flux of sputtered $B_4C$. During multilayer growth the shutter to the $B_4C$ target was kept open and the amount of $B_4C$ was controlled by the magnetron power ranging from 0 to 70W. The substrate cleaning process and other growth parameters are as described earlier [13]. A linear increase in multilayer periodicity up to 13 % was measured, upon varying the amount of $B_4C$. The obtained multilayer periods for different $B_4C$ power setting were used to adjust the growth rates for the Cr+$B_4C$ and Sc+$B_4C$ layers (see Appendix B1 for more information).

A series of five multilayers was deposited using $B_4C$ magnetron powers of 0, 34, 46, 59, and 70 W. Each multilayer contained 100 periods, and was deposited with a modulation period of $\Lambda = 1.6$ nm ( $\Gamma = d_{Cr}/\Lambda = 0.48$), appropriate for use as a normal-incidence mirror near theSc-absorption edge $\alpha\tau$ $\lambda = 3.11$ nm. Only multilayers grown without $B_4C$ or with $B_4C$ target powers > 34 W are presented here as no substantial difference was observed in hard X-ray reflectivity measurements during the optimization process among the films deposited using $B_4C$ powers between 0- 30 W. Constant ion-to-metal flux ratios of $\Phi_{Cr} \sim 4$ ions/atom and $\Phi_{Sc} \sim 8$ ions/atom were utilized and a low energy modulated ion assistance scheme

according to the following [13] was implemented. The substrate was kept grounded during the initial 0.3 nm growth of each individual layer, providing ion bombardment with energies of $E_{ion}$ (Cr) = 5.5 eV and $E_{electron}$(Sc) = -1.5 eV, and was biased with -30 V for the growth of the remaining part of each layer, providing $E_{ion}$(Cr) = 36 eV and $E_{ion}$(Sc) = 29 eV ion bombardment. As a demonstration of the optimized process, a multilayer polarizer was designed with a multilayer periodicity of $\Lambda$=2.253 nm, a layer thickness ratio, $\Gamma$ = 0.471, and N = 150 periods for reflection at the Brewster angle. The multilayer polarizer was deposited using the modulated ion assistance and uniformly incorporating $B_4C$ operated at 34 W target power. For TEM analyses a stacked multilayer structure with five different periodicities of 0.9, 1.8, 2.7, 3.6 and 4.5 nm was deposited using the same deposition parameters as for the multilayer polarizer.

To explore the effects of ion assistance simultaneous to $B_4C$ incorporation, a series of multilayers of identical design (N = 100, $\Lambda$ = 1.6 nm, and $\Gamma$=0.48, and P($B_4C$) = 34W) was grown applying three different ion energy assistances: (a) with continuous substrate bias of -30 V providing ion energies of $E_{ion}$(Cr = 36 eV, $E_{ion}$(Sc) = 32 eV, (b) at floating potential with $E_{ion}$(Cr) = 20 eV, $E_{ion}$(Sc) = 21 eV, and (c) with modulated ion assistance as described above.

### *2.2 Composition and structural characterization*

To determine elemental content in the multilayers light element sensitive Elastic Recoil Detection Analysis (ERDA), using a 40 MeV $Cl^{7+}$ beam inclined at an angle of 15° relative to the film surface, was performed [28, 29]. C *1s*, B *1s*, Cr *2p*, and Sc *2p* X-ray Photoelectron Spectroscopy (XPS) core-level spectra were acquired to analyze the chemical bonding structure of boron and carbon atoms within the layers using an Axis Ultra DLD spectrometer operating at a base pressure of $1.5\times10^{-7}$ Pa with monochromatic Al K$\alpha$ radiation (h$\nu$ = 1486.6 eV). In order to avoid uncertainties related to commonly used binding energy scale referencing against C *1s* line of adventitious carbon [30], spectra were aligned to the Fermi level cut-off. The spectra were acquired from the $0.3\times0.7$ mm$^2$ area centered at $3\times3$ mm$^2$ portion of the sample previously sputter-etched with 0.5 keV $Ar^+$ ions incident at the angle of 70° from surface normal. Deconvolution and quantification was performed using the Casa XPS software applying the manufacturer's (Kratos Analytical Ltd.) sensitivity factors [31].

The periods were determined from hard X-ray reflectivity measurements of the first order Bragg peak using Cu-K$\alpha$ radiation. The soft X-ray reflectivity was measured at the Advance Light Source (ALS) using synchrotron radiation with $\lambda$=3.11 nm, and the acquired reflectivity profiles were simulated using the IMD software [32] to estimate the average rms roughness. The polarizing properties were measured at beamline UE56/1 at BESSY II using the ultrahigh vacuum polarimeter with an energy resolution of approximately 2500 in both s and p geometries [33]. Transmission electron microscopy (TEM) imaging was performed using an FEI Tecnai G2 TF 20 UT field-emission instrument operated at 200 keV for a point resolution of 0.19 nm. For TEM, cross-sectional specimens were prepared by mechanical polishing followed by low-angle Ar ion milling.

## 3. Results and discussion

The chemical composition as determined by ERDA for a series of 5 multilayers deposited with varying $B_4C$ target powers revealed negligible amount of impurities such as H, O, and N in all multilayers (see Appendix B2). A consistent Cr/Sc ratio of 2.1 ± 0.1 was determined, whereas the B/C ratio increased from 0 to 4.13, 4.45, 4.57, and 4.61 as the $B_4C$ target power was increased from 0 to 34, 46, 59, and 70 W, respectively. The observed higher B/C ratio in the multilayers compared to the stoichiometric target is a consequence of preferential sputtering of B over C from the $B_4C$ target due to the partial sputtering yield of B being more than 4 times higher than that of C [34, 35]. Moreover, the observed increase in B/C-ratio with increasing magnetron power is likely an effect of the strong nonlinear evolution of the partial

sputtering yields of B and C, due to the significantly differing sputtering thresholds of B and C, for Ar ions in the range of ~100-200 eV. Here, we chose to the sum boron and carbon content for representation, for example the multilayer grown using a $B_4C$ magnetron power of 34 W contained 19 at.% B and 4.6 at.% C i.e., a boron-to-carbon ratio ~4.1, and thus the concentration of B+C = 23.6 at.%.

In Fig. 1(a) hard and soft X-ray reflectivity measurements of the series of five multilayers deposited with varying B+C content is shown. Each multilayer have a nominal periodicity of 1.6 nm and consists of 100 periods. Overall, a significant enhancement is seen for the first order multilayer reflections in both hard and soft X-ray reflectivity measurements. The B+C containing multilayers exhibit at least 59% increase in soft X-ray reflectivity compared to the multilayer grown without B+C (0 at.%). The highest hard X-ray intensity was measured for a multilayer containing B+C = 23.6 at.%, whereas, maximum soft X-ray reflectivity of ~12.0% was achieved for a multilayer consisting 28.0 at.% of B+C. The modulation period of the later was however slightly larger (~1.614 nm compared to the nominal periodicity of 1.60 nm), giving peak reflectance at an incidence angle of 74°. Therefore, for angular scans in Fig. 1(b), soft X-ray reflectivity is compared for the multilayer containing 23 at.% of B+C with the multilayer deposited without $B_4C$. This direct comparison reveals 67% higher reflectivity for the $B_4C$ containing multilayer. The average interface widths were 0.35 nm and 0.26 nm without and with added B+C, respectively, as estimated through simulations of the soft X-ray reflectivity. For the simulation of the B+C containing multilayers the optical constants of Cr and Sc were generated assuming 19 at.% boron and 4.6 at.% carbon in the layers (as determined by the ERDA). Bulk densities of all the elements were assumed in the simulations.

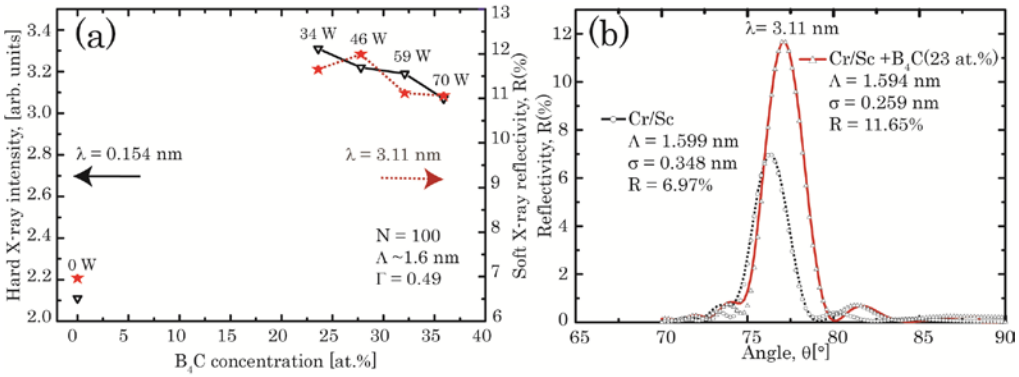


Fig. 1. (a) First order hard X-ray peak intensity and soft X-ray peak reflectivity as a function of B+C concentration. (b) Measured (symbols) and simulated (lines) soft X-ray reflectivities at λ= 3.11 nm for the multilayers without (dotted, ○) and with (solid, Δ) 23 at.% B+C.

TEM analysis of the multilayer with 23.6 at.% B+C shows that all the way up to 100 periods multilayer have smooth and well-defined interfaces (see Appendix B3). The amorphous nature of Cr and Sc layers was revealed both in high resolution imaging and selected area electron diffraction (SAED). Our previously published TEM analysis of pure Cr/Sc multilayers having similar design specifications as the present ones have shown identical layer structure and morphology [13, 36]. Since, the multilayers retain their amorphous structure in both constituent layers, independent of the amount of incorporated boron and carbon, and TEM micrographs show comparable interfacial smoothness, it is uncertain that an increased X-ray reflectivity in these multilayers is a consequence of reduced layer mixing at the interfaces due to a $B_4C$ barrier nature.

To investigate this further, the two multilayers compared in Fig. 1(b) were analysed by XPS along with a multilayer containing ~0.2 nm thin $B_4C$ layers on the top of each Cr layer. The latter multilayer was sputter deposited at CXRO by Gullikson et al. and parameters are

provided in Ref. [22, 24]. An amorphous $B_4C$ film sputter deposited on a Si(001) substrate was also included in the analysis to serve as a reference for $B_4C$ type bonding. The results are shown in Figs. 2(a-d). No significant differences in the Sc 2*p* and Cr 2*p* spectra were observed among the three Cr/Sc containing films. The two carbon containing multilayers exhibit a C *1s* peak at 282.6 eV which is characteristic of C-metal bonds [37]. However, C-B bonds can also result in a peak at a similar binding energy as the C *1s*, as is evident from the C *1s* spectrum of the $B_4C$ film [see Fig. 2(c)], which also contain a broad contribution at 284.5 eV due to C-C bonds. Hence, crucial for the characterization of a B and C bonding state is the comparison of B *1s* spectra in Fig. 2(d) which reveals clear differences. B *1s* spectrum of the $B_4C$ film contains a peak at 188.1 eV due to covalent B-C bonding [26, 38]. In contrast, corresponding spectra recorded from the Cr/Sc multilayers with either interleaved or co-sputtered B+C, exhibit a B *1s* peak at significantly lower binding energy of 187.2 ± 0.1 eV indicating higher negative charge density on B atoms with respect to that encountered in $B_4C$ reference film. This, together with much lower full-width-at-half-maximum of B *1s* peaks from the multilayers, indicates that in both cases, whether B+C is continuously sputtered or deposited as thin layers at the interfaces from the $B_4C$ target, C-metal and B-metal bonds form instead of a covalent network of B-C bonds which is supposed to act as a diffusion barrier against atomic displacements.

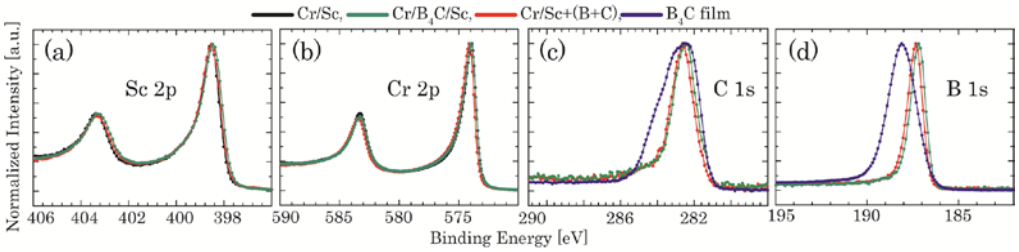


Fig. 2: (a) Sc 2p, (b) Cr 2p, (c) C 1s, and (d) B 1s core level XPS spectra of four films: the Cr/Sc (black) and Cr/Sc+$B_4C$ (red) multilayers shown in Fig. 1, Cr/$B_4C$/Sc multilayer from Ref. [22], and $B_4C$ sputtered film.

The barrier nature of $B_4C$ against intermixing was also examined by depositing a set of three multilayers with three different schemes of ion energy assistance. All multilayers contained 23 at.% of B+C and consist of 100 periods. The soft X-ray reflectivity profiles measured at $\lambda$ = 3.112 nm for the three multilayers are shown in Fig. 3. Here it is worth mentioning that highest peak reflectivities were obtained at $\lambda$ = 3.112 nm instead of $\lambda$ = 3.110 nm. Although, it is a very small wavelength shift, it does reflect dilution of the optical constants in the presence of $B_4C$. The lowest reflectivity of 7.7% is measured for the multilayer deposited using a uniform ion energies of $E_{ion}$(Cr) = 36 eV and $E_{ion}$(Sc) = 29 eV , compared to 9.2% reflectivity for the multilayer grown using uniform ion energies of $E_{ion}$(Cr) = 26 eV and $E_{ion}$(Sc) = 19 eV. This indicates an enhanced intermixing effect when using higher energy ion bombardment. During modulated ion assistance the deposition of an initial fraction of each layer with very low ion energy bombardment or electron bombardment effectively hinder kinetic surface displacements that lead to atomic scale intermixing at the interfaces. Thus, the highest reflectivity of 11.2% which is achieved for a modulated ion assistance scheme confirms that in these multilayers intermixing occur at as low energies as 20 eV and the role of $B_4C$ type bonding which supposedly isotropically limit the surface displacement is not evident. This analysis indicates that we do not have $B_4C$ covalent network and the presence of B+C, at least in the case of co-sputtered multilayers, do not play any effective role in reducing intermixing due to energetic particle bombardment.

Cr/Sc multilayers with larger periodicities, i.e., $\Lambda$>1.8 nm, exhibit higher surface roughness values originating from crystalline grain facets at the boundaries of incoherent interfaces. Thus, large period multilayers provide a suitable model to understand the influence

of $B_4C$ with respect to morphological changes, if any, inside the individual layers and at the interfaces. To work with this idea, a stack of five multilayers with different multilayer periods was deposited by co-sputtering of $B_4C$ using the same operating parameters as were used to achieve the highest reflectivity with 23.6 at.% of B+C in a single multilayer with 100 periods [Fig. 1(b)]. The number of periods were adjusted to have approximately the same total thickness of each multilayer in the stack. Fig. 4(a) shows a TEM bright field micrograph of the multilayer stack with periodicities 1.8 nm, 2.7 nm, 3.6 nm, 4.5 nm, and 0.9 nm, grown on a Si (001) substrate. The Cr (dark) and Sc (bright) layers are visible in the top four multilayers. The high resolution micrographs of these multilayers (not shown here) reveal a clear, layered structure also in the multilayer with smallest periodicity of 0.9 nm. The striking feature of the overall image is the highly defined interfaces for all multilayers and the absence of diffraction contrasts which is indicative of the presence of nm scale crystalline grains, otherwise routinely observed in large period Cr/Sc multilayers [10, 12, 13]. However, the presence of few crystallites can be seen within some areas, marked white dotted lines, of multilayers with 2.7 and 3.6 nm periods. The occurrence of this crystallization was a consequence of an unintentional interruption of the $B_4C$ flux during the deposition of these two multilayers in the stack.

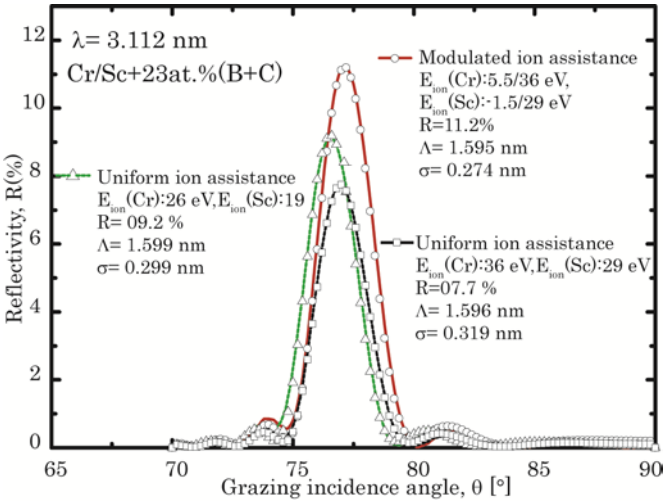


Fig. 3: Measured (lines) and simulated (symbols) reflectivity profiles performed at λ = 3.112 nm for three multilayers deposited using modulated ion assistance (solid, ○), using continuous ion assistance of $E_{ion}(Cr)$ = 26 eV, $E_{ion}(Sc)$ = 19 eV (dashed, Δ), and $E_{ion}(Cr)$ = 36 eV, $E_{ion}(Sc)$=29 eV(dotted, □). The modulation periods and average interface roughness values as determined by simulations are mentioned.

The SAED pattern of the multilayer in Fig. 4(b) shows two prominent concentric diffuse rings around the central beam, which was aligned perpendicular to the growth direction. The outer ring reflects an amorphous structure with a similar short range ordering to what is observed in SAED pattern of short period single multilayers (Appendix B3), whereas the appearance of an additional inner ring indicates the presence of long range order, although still amorphous, in large period multilayers. In addition to the diffuse rings, the SAED pattern also contain arc-shaped reflections which are indicative of preferential growth of crystallites in the growth direction. The dark field image in Fig. 4(c), obtained from the diffraction arc indicated in the figure manifest the presence of crystallites only in multilayers with 2.7 and 3.6 nm periods where $B_4C$ supply was interrupted during the growth. Depth-resolved ERDA of the multilayer stack (Appendix B2) revealed a uniform distribution of both B and C throughout the stack except, for a sharp drop in the crystalline regions shown in Fig. 4 where $B_4C$ was not incorporated during the deposition. The homogeneous distribution of boron and

carbon, independent of the interface density, shows that these atoms do not segregate to the interface layers [12]. This analysis thus shows that $B_4C$ incorporation certainly inhibits crystallite formation and promotes amorphization in both Cr and Sc layers regardless of the modulation period.

One example of an application where large period multilayers are required is for polarizing reflectors/analyzers. Fig. 5 shows the polarizing properties of a Cr/Sc+23.6 at.% (B+C) multilayer specifically design for reflection at the Brewster angle with a multilayer period of 2.26 nm and 150 periods. Bragg scans for both s and p polarized reflectivities are shown, as well as the extinction ratio i.e., $R_s/R_p$. The maxima of $R_s$ and $R_p$ appear at the Sc absorption edge due to the anomalous optical contrast at this energy. A reflectivity of 36% at incidence angle of 43.7° is achieved for s-polarized X-rays, which is an improvement of about 25% in comparison to our previously obtained result for a Cr/Sc multilayer polarizer designed without $B_4C$, giving a reflectivity of R = 26.8% at 43.7° [24, 36]. The extinction ratio $R_s/R_p$ showed a maximum of 1920 at the Brewster angle, $\theta_B$ = 44.79°, where there is a minimum in the p-polarized reflectivity, corresponding to a degree of polarization i.e. $(R_s-R_p)/(R_s+R_p)$ of 99.89 %.

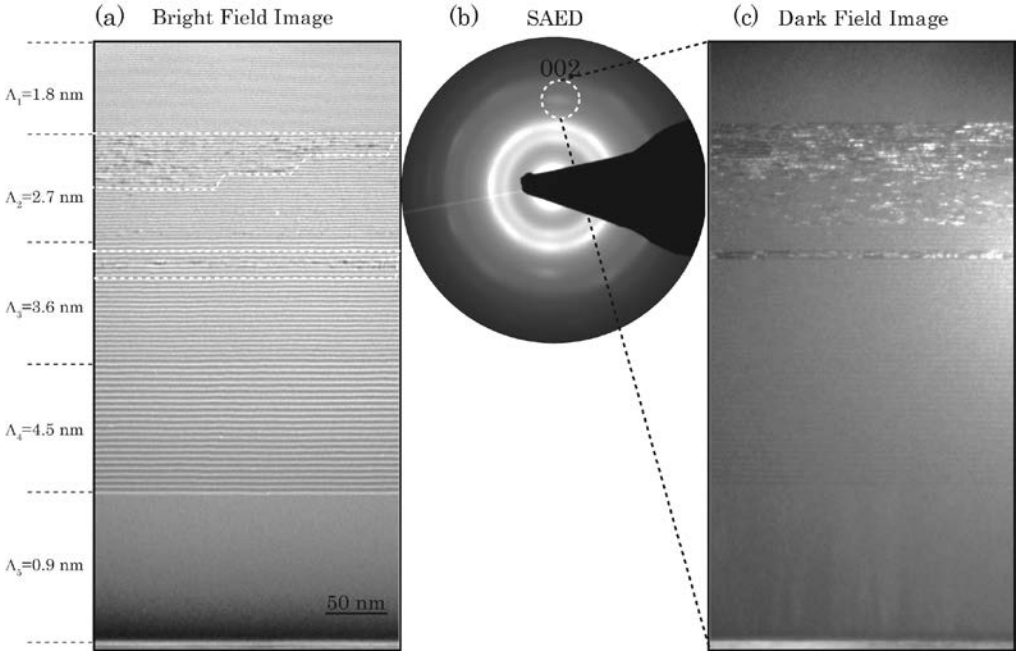


Fig. 4: TEM analysis of a Cr/Sc+(B+C) multilayer stack consisting of five multilayers with different nominal periods. (a) cross-sectional bright field micrograph, presence of areas with nanocrystallites are marked white dotted lines, (b) SAED pattern of the entire multilayer stack and, (c) the dark field micrograph recorded by selecting the average (002) reflection in the growth direction. The crystalline areas appear in both bright filed and dark field images where $B_4C$ deposition was interrupted.

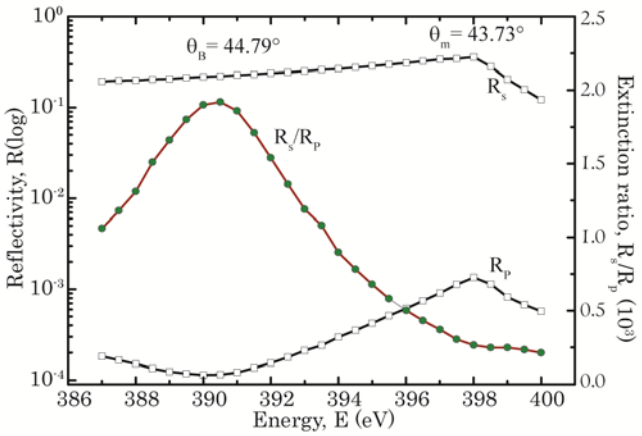


Fig. 5. Polarizing properties of Cr/Sc+23.6 at.%(B+C) multilayer with Λ = 2.26 nm and N = 150. Bragg scans for s- and p-polarizing geometries ($R_s$, $R_p$) and extinction ratios ($R_s/R_p$) are shown. $\theta_B$ is the measured Brewster angle and at $\theta_m$ indicates maximum s-component of the reflectivity.

## 4. Discussion and final remarks

The $B_4C$ co-sputtered multilayers are conceptually incomparable to the interleaved $B_4C$ diffusion barrier layers in terms of optical contrast and hindrance mechanism for intermixing at the interfaces. However, XPS analysis infer that in both multilayers there is a higher negative charge density on B atoms than what is expected from covalent B-C bonding. This suggests that instead of forming a covalent network of B-C bonds which act as diffusion barrier against atomic displacements, sputtered carbon and boron atoms preferably bind to metal atoms at the growing surface, even in the case of interleaved $B_4C$ layers. Despite the fact that no $B_4C$ bonds were detected, the two Cr/Sc multilayer coating designs, i.e., the one with interleaved B+C layers on the top of each Cr layer [22] and the one with homogeneously distributed B+C (this work) resulted in high quality multilayers. In the later 67% increase in soft X-ray reflectivity is achieved on incorporating 23.6 at.% of B+C compared to the multilayer grown without $B_4C$.

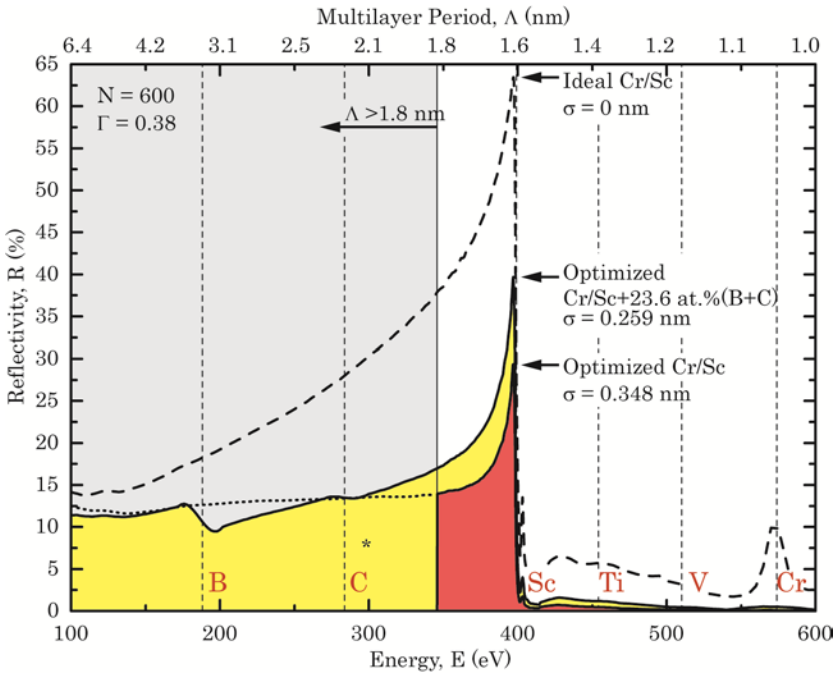


Fig. 6. Predicted reflectivity performance in the energy range 100 - 600 eV for Cr/Sc and Cr/Sc:$B_4C$ multilayers containing N=600 periods and layer thickness ratios of 0.38. The interface widths used for the calculations are the same as those obtained in the reflectivity simulations in Figure 1, i.e, $\sigma$ = 0.348 nm for Cr/Sc and 0.259 nm for Cr/Sc:(B+C). The theoretical limit is indicated by a dashed line for an ideal Cr/Sc multilayer. *marks state-of-the-art reflectivity R=8%, at 300 eV [19]

We conclude that increased X-ray reflectivity in the multilayers is primarily due to a B+C driven amorphization resulting into smoother interfaces. Without B+C, the spontaneous amorphization of Cr and Sc layers in short period ($\Lambda$ < 1.8 nm) multilayers is a consequence of a high density of atomically disordered interfaces, and the disorder is there to lower the system total energy compared to forming coherent crystalline interfaces. That is why nanocrystalline layers emerge upon lowering the interface density. The two aspects associated with such an amorphization are; (i) it is unstable as it is layer thickness dependent, and (ii) there is an intrinsic interface width associated with disorder interfaces. In B+C co-sputtered multilayers the major effect of B-metal and C-metal bonding is that it stabilizes a “real” amorphous structure in both Cr and Sc layers independent of layer thickness and thus provides smoother interfaces. Moreover, lower diffusivities of metal atoms bonded with B and C atoms also hinder intermixing of the layers, to some extent, although this effect is not pronounced. We found that intermixing occur at higher ion bombardment, $E_{ion}$ > 20 eV, and the modulated ion assistance scheme is beneficial to obtain abrupt interfaces.

We believe that for the Cr/Sc multilayers with interleaved B+C layers, the above mention effect of interface smoothness through stabilized amorphization also plays a major role rather than interface abruptness obtained through $B_4C$ diffusion barriers. However, to confirm the later, one has to investigate effect of different ion assistance schemes in these multilayers.

In summary, the effect of B+C in stabilizing amorphous multilayers, with smoother interfaces and reduced roughness accumulation, independent of thickness is extremely beneficial in fabricating large period multilayers. Substantially enhanced reflective properties for the long wavelength spectrum of soft X-rays and EUV radiation can be achieved. However, depending on the chosen materials and operating wavelengths of interest, one has to be aware

of the variation in optical contrast originating from B+C incorporation. In the case of Cr/Sc, calculations reveal that more than 12% normal incidence reflectivity over an extended soft X-ray wavelength range is attainable. This is illustrated in Fig. 6, where simulated normal incidence reflectivities of infinite stack (N = 600) of ideal Cr/Sc multilayers are plotted in the soft X-ray energy range 100 – 600 eV, including the Sc absorption edge at about 399 eV. For the calculations it is assumed the interface width obtained for N=100 periods can be maintained throughout a multilayer consisting of N=600 periods. Also indicated in the plot are various absorption edges of other transition metals as well as the light elements like B and C. For Cr/Sc multilayers without B+C, periods above 1.8 nm (region marked in grey) the layers are nanocrystalline with large interface widths and no reflectivity as a result. The dashed line for the Cr/Sc reflectivity curve corresponds to an imaginary calculated reflectivity in case an interface width of 0.348 nm could be maintained. The small peak above the Sc absorption edge is a result of the appearence of the refractive index of Sc at this energy. It can be noted that the attainable reflectivity from Cr/Sc:B+C(23.6 at.%) multilayers is always higher than for Cr/Sc. The reduced optical contrast due to the introduction of B and C into the structure is more than well compensated for by the reduced interface roughness provided by the amorphization of the layers. It is clear that the presence of B and C edges affect the reflective properties of Cr/Sc+(B+C) multilayers in this region. Similar calculations can be performed for other material systems and competing effects of roughness reduction due to amorphization and optical constant variation can be trade off by choosing the appropriate amount of B+C.


## Acknowledgments

We acknowledge Dr. J. Jensen and Dr. C. Höglund for the assistance in ERDA measurements, and P. Larsson for technical help in updating the deposition system.

## Funding

The authors acknowledge financial support from the Swedish Science Council and the Swedish Government Strategic Research Area in Materials Science on Functional Materials at Linköping University (Faculty Grant SFO-Mat-LiU No 2009 00971).

## Appendix B1

Multilayer period variation as a function of $B_4C$ target power.(see Fig. 7)

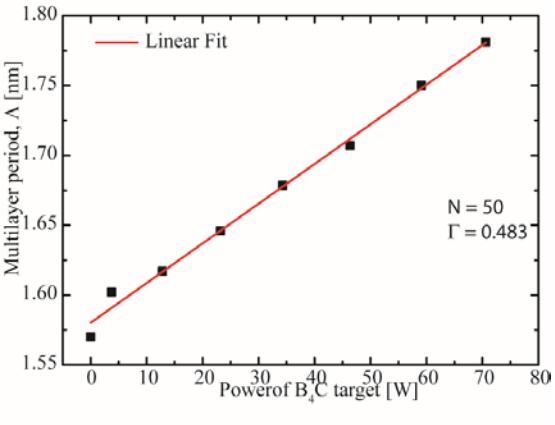


Fig. 7: Multilayer period variation as a function of $B_4C$ target power. Period (squares) is determined from HXR reflectivity IMD- simulations of multilayers deposited with varying power. Red line is linear fit to the data..

## Appendix B2

Cross sectional TEM image of the Cr/Sc multilayer (See Fig.8)

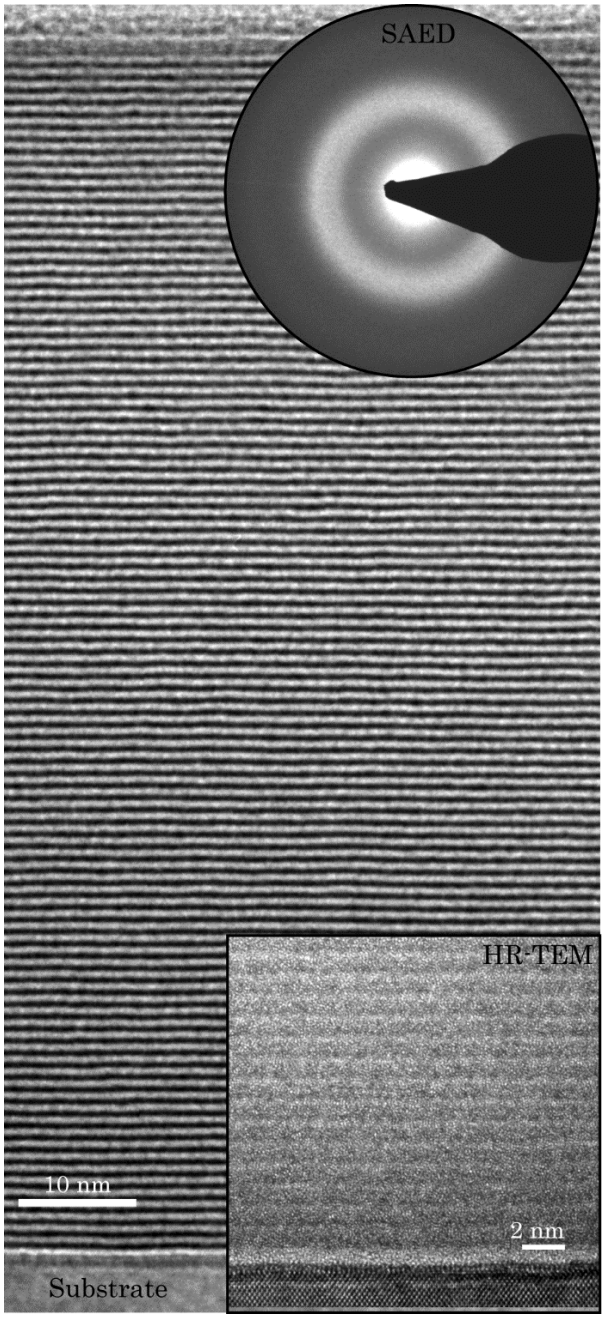


Fig. 8: Cross sectional TEM image of the Cr/Sc multilayer containing 23 at.% of B+C and exhibing 11.65 % reflectivity at Sc edge. In the upper inset SAED magnified around the central electron beam is shown. The lower inset shows the high resolution image of the substrate and the bottom of the multilayer stack.

## Appendix B3

Depth resolved ERDA of Cr/Sc+$B_4C$ multilayers (See. Fig. 9)

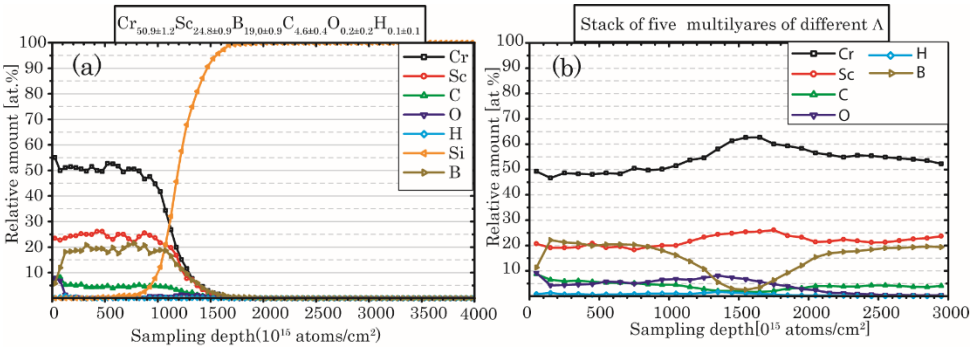


Fig. 9: ERDA results**,** **(**a) For Cr/Sc multilayer containing 23 at.% of B+C and exhibiting 11.65 % reflectivity at Sc edge. (b) Depth resolved ERDA of Cr/Sc+$B_4C$ multilayer stack constituting five multilayers of different nominal periods.